

Article

Hydrophilized MoS₂ as Lubricant Additive

M. Humaun Kabir ¹, Darrius Dias ², Kailash Arole ¹ , Reza Bahrami ¹ , Hung-Jue Sue ¹ and Hong Liang ^{1,2,*} 

¹ Department of Materials Science and Engineering, Texas A&M University, College Station, TX 77843-3127, USA; mkhumaun@tamu.edu (M.H.K.); kailash_arole@tamu.edu (K.A.); reza.bahrami@tamu.edu (R.B.); hjsue@tamu.edu (H.-J.S.)

² J. Mike Walker '66 Department of Mechanical Engineering, Texas A&M University, College Station, TX 77843-3123, USA; djdias2000@tamu.edu

* Correspondence: hliang@tamu.edu

Abstract: Molybdenum disulfide (MoS₂) has been used in a variety of lubrication products due to its highly tunable surface chemistry. However, the performance of MoS₂-derived tribofilms falls short when compared to other commercially available antiwear additives. The primary objective of this study is to improve the tribological performance of MoS₂ as an additive for lithium-based greases. This was achieved by functionalizing the particle with hydrophilic molecules, such as urea. Experimental results indicate that the urea-functionalized MoS₂ (U-MoS₂) leads to a notable decrease in the coefficient of friction of 22% and a substantial reduction in the wear rate of 85% compared to its unmodified state. These results are correlated with the density functional theory (DFT) calculation of U-MoS₂ to theorize two mechanisms that explain the improved performance. Urea has the capability to reside both on the surface of MoS₂ and within its interlayer spacing. Weakened van der Waals forces due to interlayer expansion and the hydrophilicity of the functionalized U-MoS₂ surface are catalysts for both friction reduction and the longevity of tribofilms on hydrophilic steel surfaces. These findings offer valuable insights into the development of a novel class of lubricant additives using functionalized hydrophilic molecules.

Keywords: MoS₂; functionalization; lubricant; hydrophilic; friction; additives



Citation: Kabir, M.H.; Dias, D.; Arole, K.; Bahrami, R.; Sue, H.-J.; Liang, H. Hydrophilized MoS₂ as Lubricant Additive. *Lubricants* **2024**, *12*, 80. <https://doi.org/10.3390/lubricants12030080>

Received: 23 January 2024

Revised: 26 February 2024

Accepted: 28 February 2024

Published: 5 March 2024



Copyright: © 2024 by the authors. Licensee MDPI, Basel, Switzerland. This article is an open access article distributed under the terms and conditions of the Creative Commons Attribution (CC BY) license (<https://creativecommons.org/licenses/by/4.0/>).

1. Introduction

Friction and wear in machinery leads to energy waste and a decrease in the operational lifespan of equipment [1]. A method to counteract this is the development of effective lubricants to minimize the impact of friction and wear within a moving system. Grease is classified as a semi-solid lubricant, containing a base oil, thickener, and additives [2]. They can adhere more effectively to surfaces, offering diverse functionalities while safeguarding against friction [3,4]. Tremendous efforts have been directed toward improving grease performance through the incorporation of various additives. Amongst these, the inclusion of two-dimensional (2D) materials, such as graphene, boron nitride, Mxenes, zirconium phosphate, and MoS₂, has garnered considerable interest [5–8]. This is primarily ascribed to the distinctive characteristics exhibited by these materials, such as their high-strength layered structure, low friction, and enhanced resistance to wear [9–12].

The tribological performance of MoS₂ is attributed to the presence of covalently bonded hexagonal lamellar structures, wherein the layers are joined by a weak van der Waals attraction force, resulting in low shear strength [13]. This characteristic facilitates the sliding of these layers and their deposition onto a substrate, effectively lowering the coefficient of friction and promoting the formation of a tribofilm to reduce wear. It has previously been employed as a solid lubricant and an extreme pressure additive in a variety of greases [14–17]. However, the development and durability of a MoS₂-derived tribofilm falls short when compared to commercially available antiwear additives like Zinc dithiophosphate (ZDDP) [18,19]. ZDDP exhibits an inherent polarity in its molecular

structure, enabling it to establish spontaneous interactions with a metal surface. In contrast, MoS₂ consists of a hexagonal arrangement of molybdenum atoms, surrounded by nonpolar sulfur atoms in a sandwich-like configuration. Inconsistencies in the performance of MoS₂ can be ascribed to its vulnerability to environmental influences. Research findings have indicated that MoS₂ adsorbs moisture present in the surrounding environment, initiating its oxidation [20,21]. Water, as a small molecule, has the ability to intercalate between the layers of MoS₂, resulting in the generation of an attractive force that hinders interlayer sliding [22–24].

One effective approach to enhance the durability of tribofilms and to promote prolonged interactions with the surfaces in contact is through the functionalization of MoS₂ using polar molecules [25,26]. In addition, the process of microencapsulation of MoS₂ delivers the advantage of shielding MoS₂ from moisture absorption in a humid environment, as well as preventing its oxidation when subjected to frictional loads [27]. Another benefit of utilizing functionalized molecules is their ability to intercalate between layers, increasing interlayer spacing and reducing the Van der Waals attraction force [28,29]. The decrease in the force of attraction facilitates the movement of these layers, enabling them to slide and spread more evenly throughout the surface area in contact [29,30].

In the present investigation, urea was designated as the functionalized molecule, relying on its environmentally friendly nature, thermal stability, and notably its hydrophilic characteristics resulting from the presence of two amine groups connected to a carbonyl group [31,32]. The objective of our research was to employ urea molecules as a means to modify the surface of MoS₂ and improve its tribological properties. A simple one-step synthesis process was explored for the preparation of urea-functionalized MoS₂ (U-MoS₂). A thermogravimetric analysis (TGA) and X-ray diffraction (XRD) were conducted in order to confirm the presence of urea. Additionally, a water dispersibility test was carried out to validate any surface modifications of MoS₂ caused by the presence of urea. Furthermore, to conduct a comparative analysis of the tribological performance of MoS₂ and U-MoS₂, an investigation was carried out to evaluate the coefficient of friction (COF) and observe the wear patterns on the worn surface. Afterward, to verify the adsorption and intercalation potential of urea with MoS₂ crystals, density functional theory (DFT) simulations were performed. Possible structural changes in MoS₂ crystals after urea intercalation were assessed to validate their potential to improve tribological performance.

2. Materials and Methods

2.1. Materials and Sample Preparation

Urea (ACS reagent, 99–100.5%), Molybdenum (IV) disulfide (<2 μm, 98%), and 2-propanol (anhydrous, 99.5%) were acquired from Sigma Aldrich (St. Louis, MO, USA). The lithium base grease was supplied by Chemtool Incorporated (Rockton, IL, USA).

A simple adsorption reaction was conducted to investigate the influence of urea on the MoS₂ material. Initially, a quantity of 0.2 gm of urea was dissolved in 2-isopropanol and thereafter subjected to stirring for 30 min. Subsequently, MoS₂ was introduced into the solution, ensuring a molar ratio of 1:1 with respect to the concentration of urea. It is important to note that the ratio of urea and MoS₂ was adjusted from 0.5:1 to 1.5:1, with the 1:1 ratio identified as optimal for transitioning the MoS₂ particles from hydrophobic to hydrophilic based on the water dispersibility test. Furthermore, the reaction was allowed to proceed under continuous magnetic stirring for 24 h at a temperature of 40 °C. Afterward, the particles were extracted from the solution using a centrifuge machine, followed by several washes with acetone to eliminate any remaining urea residues. Subsequently, the particles underwent a drying process at a temperature of 50 °C for 6 h within ambient atmospheric conditions.

2.2. Characterization

Thermogravimetric analysis (TGA) was examined by using a TA instruments (New Castle, DE, USA) SDT: Q600 thermal analyzer. The sample was heated at a rate of 10 °C/min,

starting from room temperature and progressing up to 500 °C. X-ray powder diffraction (XRD) was utilized to characterize the samples using a Bruker (Billerica, MA, USA) D8 powder X-ray diffractometer incorporated with a LynxEye detector in the Bragg–Brentano geometry equipped with Cu K α radiation ($\lambda = 1.54178 \text{ \AA}$). The morphology of MoS₂ and U-MoS₂ was observed with a VEGA field-emission scanning electron microscope manufactured by TESCAN (Brno, Czech Republic). An imaging acceleration voltage of 10 kV was employed, and the conducting carbon tape was placed in a sample holder to hold the samples for testing. Moreover, the water dispersibility test was used to identify the hydrophilic nature of the particles. To do so, a 0.1 M solution was prepared and subjected to ultrasonication for 30 min at room temperature to ensure thorough mixing and dissolution.

2.3. Tribotesting

The tribological performance was evaluated by employing particles of urea, MoS₂, and U-MoS₂ as an additive with lithium base grease, with a concentration of 0.25 wt.%. The friction and wear tests were conducted with an Anton Paar (Graz, Austria) manufactured TRB³ Pin-on-disk tribometer. The arrangement consisted of an AISI 4130 low-carbon steel plate and an AISI E52100 steel ball with a diameter of 6.35 mm. Prior to commencing the tests, a thin coating of the prepared grease, approximately 1 mm in thickness, was applied onto the steel substrate. A reciprocating motion was established with a velocity of 5 cm/s and a maximum amplitude of 6 mm. Three distinct loading conditions (5 N/10 N/15 N) were subsequently applied to the surface throughout the experiment. Each test was repeated a minimum of three times in order to determine the most accurate performance of these particles.

The wear profiles were analyzed by a 3D surface profiler (VK-9700) manufactured by Keyence Corporation of America (Itasca, IL, USA). A minimum of six distinct cross-sectional profiles were evaluated to calculate the average cross-section of the wear track. The wear rate, denoted as K , was determined using the following equation [33]:

$$K = \frac{V}{Ld} \quad (1)$$

Here, V defines the wear volume of the worn surface, L is the applied load, and d represents the total sliding distance throughout the test.

2.4. DFT Simulation

The investigation of the geometrical changes resulting from the intercalation of urea within the MoS₂ layers was carried out by DFT simulations utilizing the open-source software Quantum ESPRESSO ver. 6.6 [34]. In this study, a $2 \times 2 \times 2$ supercell was utilized to examine the MoS₂ model, which consisted of four layers. The placement of the urea molecule within the supercell was performed in a manner that aligned it parallel to the atomic layers of MoS₂. The core electrons were defined using ultrasoft pseudopotentials, and the exchange-correlation energy was demonstrated using the generalized gradient approximation (GGA) as per Perdew–Burke–Ernzerhof (PBE) [35]. A dense Monkhorst–Pack with grids of $5 \times 5 \times 1$ was used to define the Brillion zone. In addition, the cutoff energy of 50 Ry was selected with an energy convergence threshold of 10^{-6} eV and a force convergence requirement of 10^{-4} eV \AA^{-1} .

The adsorption energy was determined by utilizing a 4×4 MoS₂ sheet as the substrate, onto which a urea molecule was positioned parallel to the hexagonal layers of MoS₂. The unit cell was periodic in both the x and y planes, while a vacuum region of 20 \AA was established in the z direction along the (002) plane to prevent any interaction between adjacent cells. The adsorption energy (E_{ads}) was estimated by using the following equation [32]:

$$E_{ads} = E_{MoS_2+Urea} - E_{MoS_2} - E_{Urea} \quad (2)$$

where $E_{\text{MoS}_2+\text{Urea}}$ denotes total energy associated with the urea adsorbed onto the MoS_2 substrate. E_{MoS_2} and E_{Urea} define the energy of an isolated MoS_2 layer and an isolated urea molecule, respectively.

3. Results and Discussion

3.1. Morphology of Urea- MoS_2

Urea molecules are first attracted to the surface of MoS_2 particles through an adsorption mechanism that yields U- MoS_2 . In order to determine the presence of functionalized urea, thermal gravimetric analysis (TGA) was conducted through a temperature range spanning from ambient conditions to 500 °C. The weight loss around 100 °C, as depicted in Figure 1a, was found to be the most significant in ideal conditions. This weight loss can be attributed to the removal of water molecules trapped between MoS_2 layers. The introduction of moisture into the interlayers of MoS_2 leads to the initiation of particle oxidation and subsequent degradation of its lubricating performance [24]. On the other hand, a significant reduction in weight was seen in U- MoS_2 , commencing at approximately 150 °C and persisting until 350 °C. This phenomenon can be attributed to the inclusion of urea inside the structure, as reported in a previous study [36]. Interestingly, the weight loss of U- MoS_2 was much lower than MoS_2 at temperatures approaching 100 °C. This observation provides evidence that urea can effectively displace moisture in MoS_2 and serve as a protective agent against oxidation [27]. Furthermore, XRD patterns were analyzed to identify the crystal structures of MoS_2 and U- MoS_2 , as depicted in Figure 1b. The diffraction peaks demonstrate the phase purity of MoS_2 , which possesses a hexagonal structure, specifically the 2H phase as identified by the JCPDS card no. 37-1492 [37,38]. It is worth noting that this hexagonal structure remains unaffected even after the modification by urea. The peaks of U- MoS_2 shift from 14.4° to 14.1°, indicating an expansion of the interlayer spacing. The decrease in peak intensity, approximately 18 %, appears to be associated with the decrease in crystallinity, which is a consequence of the integration of urea into the structural matrix of MoS_2 .

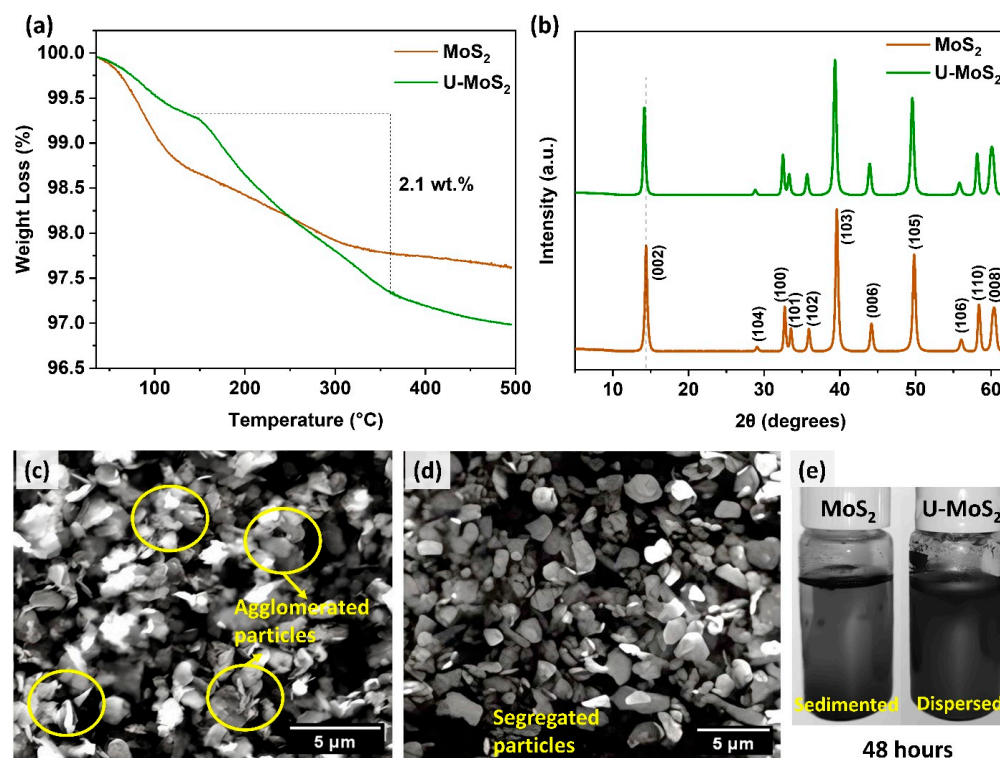


Figure 1. (a) Thermogravimetric analysis; (b) XRD data of MoS_2 and U- MoS_2 ; SEM images of (c) MoS_2 and (d) U- MoS_2 ; (e) water dispersion test of MoS_2 and U- MoS_2 .

The identification of the morphology and microstructure of these particles was conducted using a scanning electron microscope (SEM). The dispersion and separation of U-MoS₂ particles were evident when comparing them to the agglomerated MoS₂ particles, as depicted in Figure 1c,d. The functionalization of particles with urea hinders their tendency to agglomerate to the particles of MoS₂, hence offering advantages in enhancing tribological performance. In order to assess the surface characteristics of U-MoS₂, a water dispersibility test was conducted. As shown in Figure 1e, dispersion of MoS₂ tends to precipitate within a few hours and completely sediment less than 48 h. This is attributed to the hydrophobic nature of MoS₂ due to nonpolar sulfur elements in the structure [39–41]. In contrast, U-MoS₂ was uniformly dispersed in water throughout the time due to its hydrophilic nature [27,33,42].

3.2. Tribological Performance

The particles of MoS₂ and U-MoS₂ were incorporated as additives into a lithium base grease to perform their tribological tests. MoS₂ can generate a tribofilm when subjected to friction, resulting in the maintenance of a low coefficient of friction (COF) [18,43,44]. Formation and removal of tribofilm is a continuous process, characterized by a higher formation rate initially, followed by attaining an equilibrium state after a specific duration and subsequently reaching a lower formation rate than the removal rate, which signifies a deterioration in lubricating performance [18,45].

The coefficient of friction (COF) was measured for four thousand cycles under the 5N load to evaluate the impact of MoS₂ and urea molecules as compared to base grease. Initially, the COF for lithium grease exhibited a higher value, as depicted in Figure 2a, which gradually diminished as the cycle count increased. The pattern for urea-grease mirrors this, albeit with marginally lower values, suggesting that urea's sole contribution to friction reduction is minimal. In contrast, the COF for both MoS₂ and U-MoS₂ remained consistently lower throughout the testing period, highlighting MoS₂'s effectiveness in enhancing the tribological performance of base grease. Figure 2b presents the average COF for all samples, with U-MoS₂ recording the lowest, underscoring the synergistic effect of combining urea with MoS₂ to boost performance.

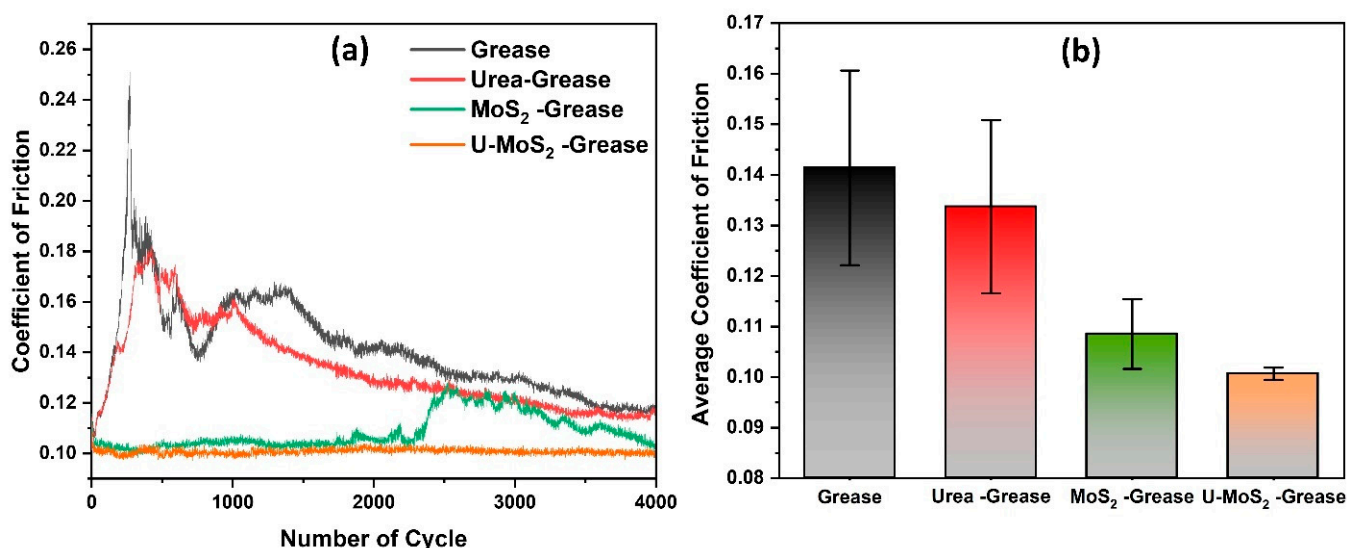


Figure 2. (a) Variation of coefficient of friction (COF) and (b) average friction coefficient for grease, urea-grease, MoS₂-grease, and U-MoS₂-grease at 5N applied load.

Three different loads were applied on the surface to assess the tribological performance of MoS₂ and U-MoS₂, focusing on their ability to maintain the tribofilm and the subsequent impact on wear rate. The response of MoS₂ and U-MoS₂ under an applied load of 5 N is illustrated in Figure 3a. It is observed that MoS₂ exhibits a low COF until 2300 cycles; how-

ever, the COF subsequently increases due to the breakdown of the tribofilm. Conversely, U-MoS₂ demonstrated a consistent and low COF throughout the entire test. According to previous research [46], it is anticipated that the friction force will exhibit a proportional rise in response to an increase in the normal load, hence maintaining a constant COF. However, in Figure 3b, the COF of MoS₂ fluctuates wildly after just 270 cycles under the increased loading condition of 10N. This is perceived to be due to the removal rate of the tribofilm outpacing its formation rate at several instances during the test [18] and the lower dispersibility of unmodified MoS₂ due to their increased agglomeration, as seen in Figure 1. In contrast, U-MoS₂ demonstrated a nearly constant COF until 2500 cycles, at which point the lubricating effect of the tribofilm formation reaction reached a new stable equilibrium.

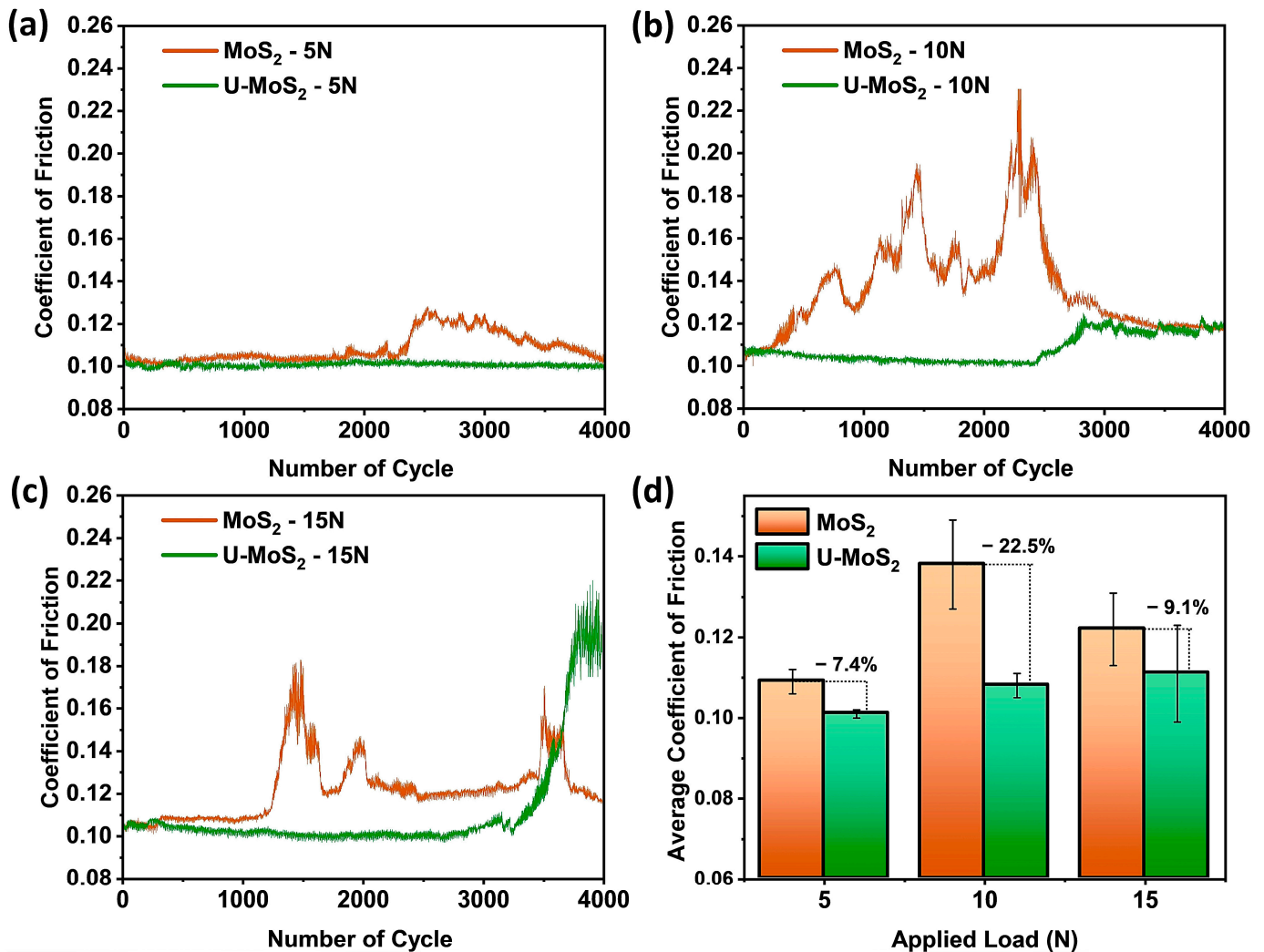


Figure 3. Variation of coefficient of friction (COF) for the different applied loads of (a) 5N, (b) 10N, and (c) 15N; (d) average COF with three applied loads for MoS₂ and U-MoS₂.

Furthermore, it is noteworthy to add that the tribofilm can increase its thickness and also achieve a more compact structure due to the initial generation of a large amount of wear debris under an increased applied load [47,48]. This can be used to explain the eventual decrease in the COF of MoS₂ for 10 N to eventually reach parity with the COF of U-MoS₂ after 2800 cycles. In Figure 3c, the COF of MoS₂ fluctuates again as in the previous case but remains consistently above the COF of U-MoS₂ for a majority of the test. At around 3248 cycles, the increased loading condition of 15 N takes its toll on the U-MoS₂ and causes it to break down completely before it begins to recover at around 4000 cycles. In Figure 3d, we can observe that the initial COF has a positive correlation with the applied load, leading

to an increase in the diameter of the wear scar, ultimately resulting in a reduction in the applied pressure under the contact due to the continuously increasing contact area. This is evidenced by the performance advantage of the COF of U-MoS₂ against the COF of MoS₂ being lower for the 15 N load in comparison to the 10 N load. Overall, it can be observed that the COF of U-MoS₂ was consistently lower than that of pure MoS₂ across all scenarios. This finding suggests that the introduction of urea to functionalize MoS₂ can enhance the longevity of tribofilm reactions when compared to the unmodified particles.

The characteristics of wear are correlated with the processes of tribofilm formation and removal [18,19]. Figure 4 illustrates the three-dimensional wear profiles of MoS₂ and U-MoS₂ when subjected to varying applied stresses. The wear tracks of both materials exhibited an increase in the local surface roughness of the wear track when the applied load was increased, characterized by the presence of a more pronounced wear scar. In all instances, it was noticed that MoS₂ created deeper and rougher grooves in comparison to U-MoS₂. This finding suggests that the surface formation due to the presence of U-MoS₂ exhibited a significantly higher level of smoothness when compared to MoS₂, which can be attributed to the existence of their respective tribofilms.

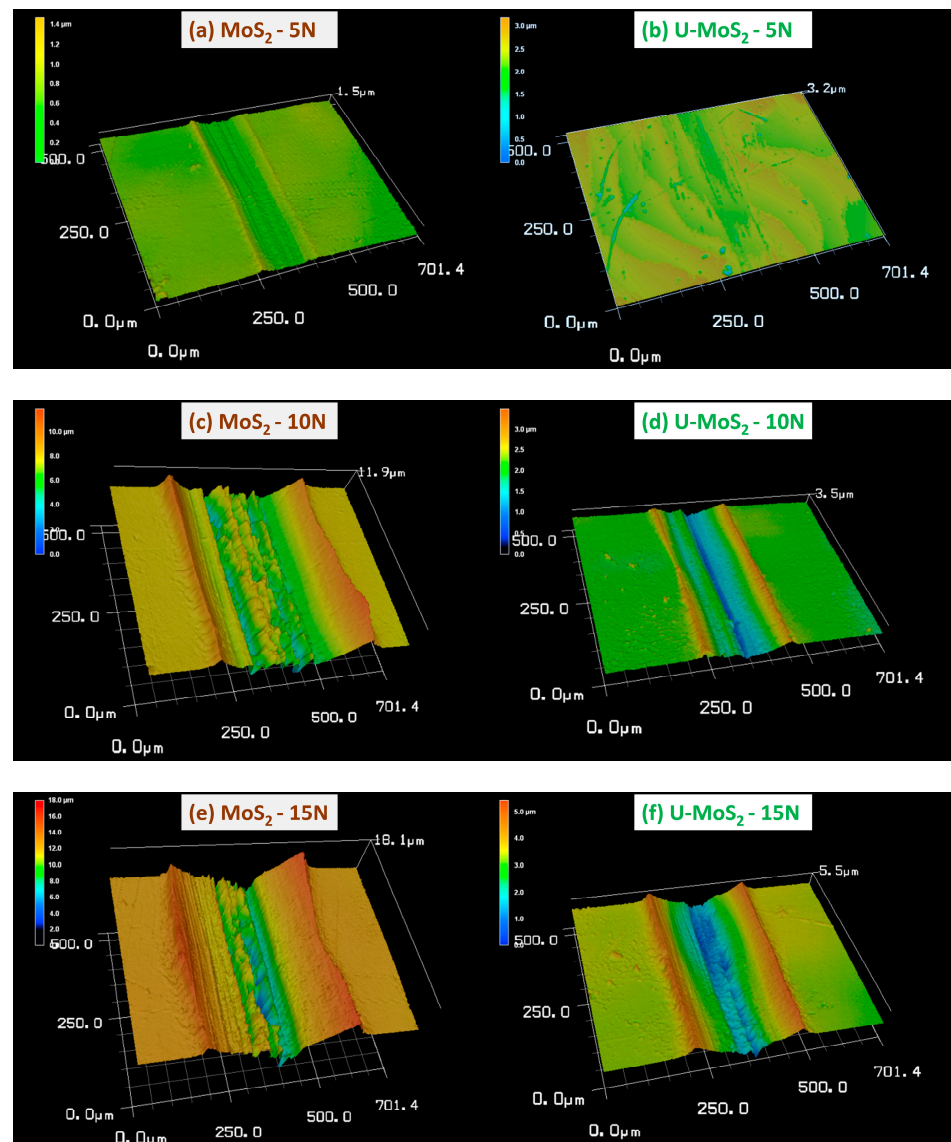


Figure 4. Three-dimensional profiles of wear track of MoS₂ and U-MoS₂ under normal loads for (a,b) 5 N, (c,d) 10 N, and (e,f) 15 N, respectively.

Figure 5 depicts a quantitative analysis of the wear performance exhibited by MoS₂ and U-MoS₂. The scar diameter increased with increasing applied normal load for both materials, as shown in Figure 5a. However, it is worth noting that the rate of growth in scar diameter was significantly lower for U-MoS₂ compared to MoS₂. The findings pertaining to scar depth, as illustrated in Figure 5b, exhibit comparable patterns. The wear track depth for MoS₂ under a normal load of 15 N was found to be 9.5 μm , which was the greatest among the tested samples. In contrast, U-MoS₂ exhibited a wear track depth of just 3.7 μm . Figure 5c,d depicts the wear volume and the associated wear rate of the samples. The wear volume of U-MoS₂ is substantially lower than that of MoS₂, indicating the enhanced performance of tribofilms when MoS₂ is functionalized with urea molecules. It is noteworthy to highlight that the observed pattern of wear rate variation in relation to the applied load, as portrayed in Figure 5d, bears a resemblance to the average coefficient of friction, as depicted in Figure 3d. The tests with lower average COF resulted in lower average wear rates and less severe wear scars.

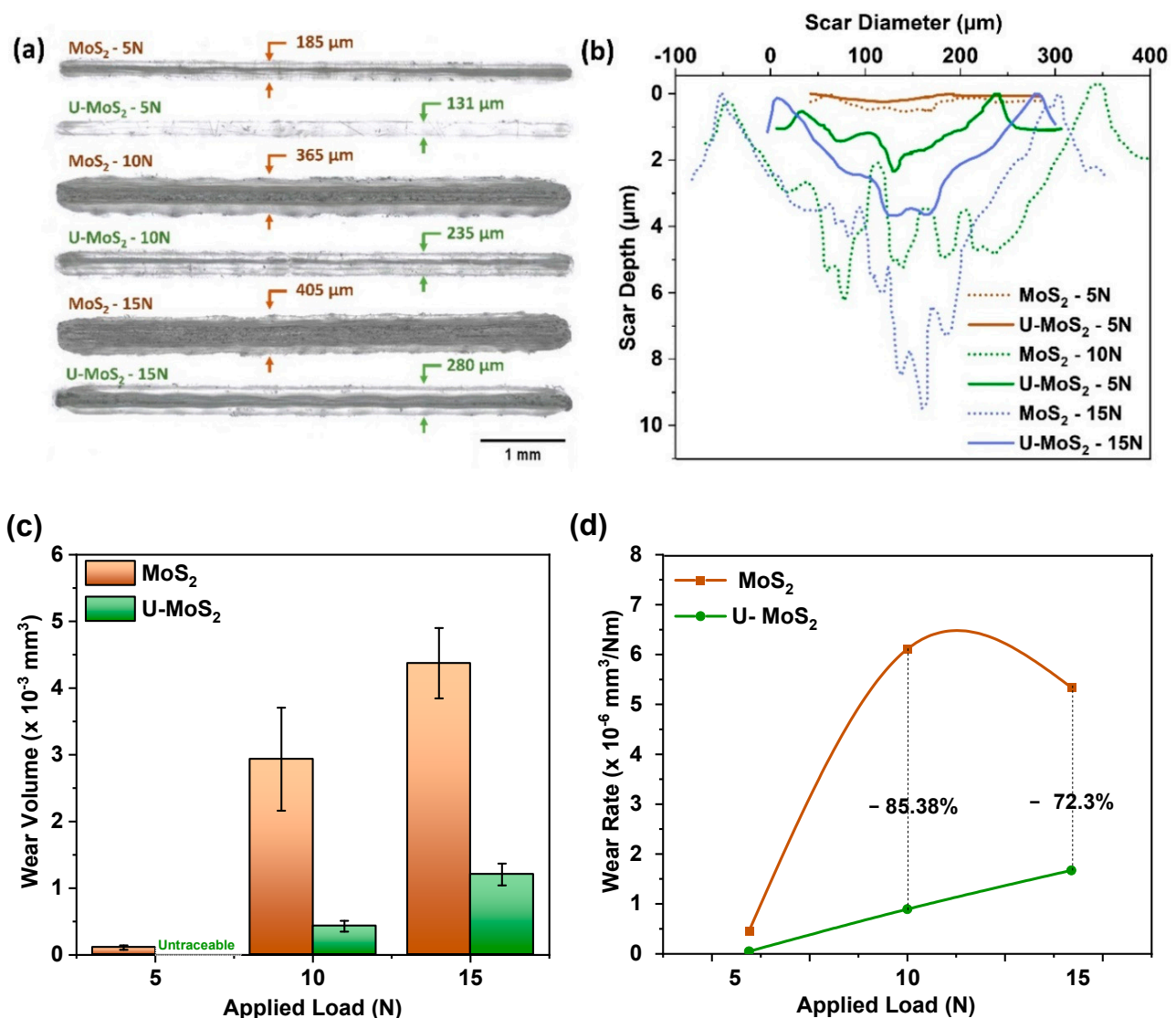


Figure 5. Wear (a) track, (b) depth profile, (c) volume, and (d) rate of MoS₂ and U-MoS₂ under the different normal loads.

The surface morphology of the wear track was scrutinized to elucidate the superior performance of U-MoS₂, as illustrated in Figure 6. SEM imagery revealed a smooth tribofilm within the wear track, which likely contributed to the observed low COF and wear rate.

EDS mapping indicated a uniform distribution of MoS₂ across the surface, along with notable carbon presence. The tribofilm is primarily composed of nitrogen and oxygen, signifying its composition largely of oxide and nitride compounds. Notably, urea molecules are composed of nitrogen, carbon, and oxygen, which facilitates the formation of nitride, oxide, and carbide compounds with molybdenum and iron, crucial for reducing wear rate during frictional interactions.

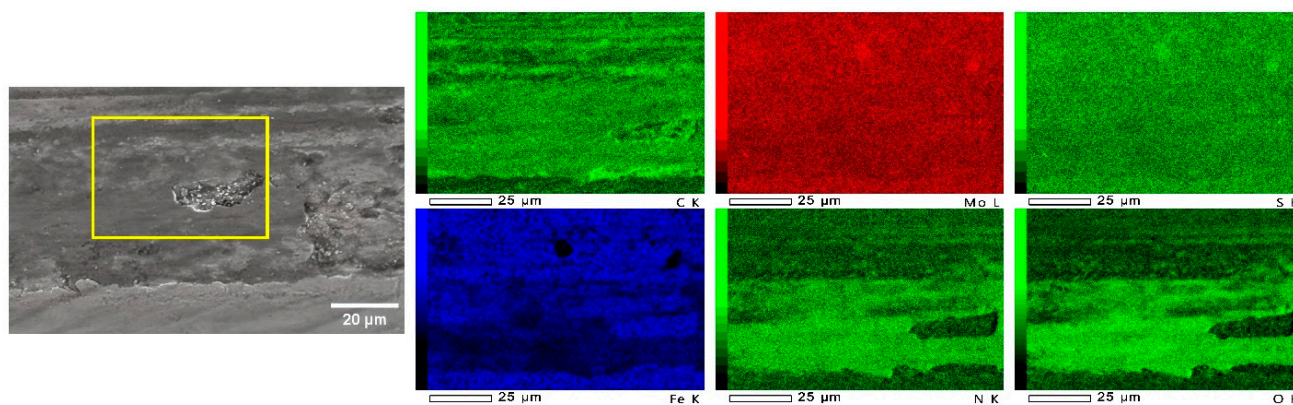


Figure 6. SEM image of wear track of U-MoS₂ and its corresponding EDS mapping.

3.3. Crystal Structure of U-MoS₂

The 2H-MoS₂ crystal structure was considered for DFT simulations based on its superior thermodynamic stability in comparison to the alternative polymorphs, namely 1T-MoS₂ and 3R-MoS₂ [49,50]. Also, the XRD results revealed that the crystal structure of MoS₂ exists in the 2H phase. 2H-MoS₂ is mainly a hexagonal structure (space group P6₃/mmc), which consists of A-B-A-B stacking sequences with edge-sharing [MoS₆] trigonal prisms [51,52]. In the MoS₂ structure, urea molecules are positioned in two distinct ways: intercalation between the MoS₂ layers and adsorption on the MoS₂ surface. Earlier studies have demonstrated that the optimal alignment of the urea molecule with hexagonal layered materials occurs when it is parallel to the (002) direction [32,36,53,54]. Taking this into account, the spatial arrangement is illustrated in Figure 7, highlighting the parallel alignment of the urea molecules to the MoS₂ layers, indicative of their interaction dynamics within the structure.

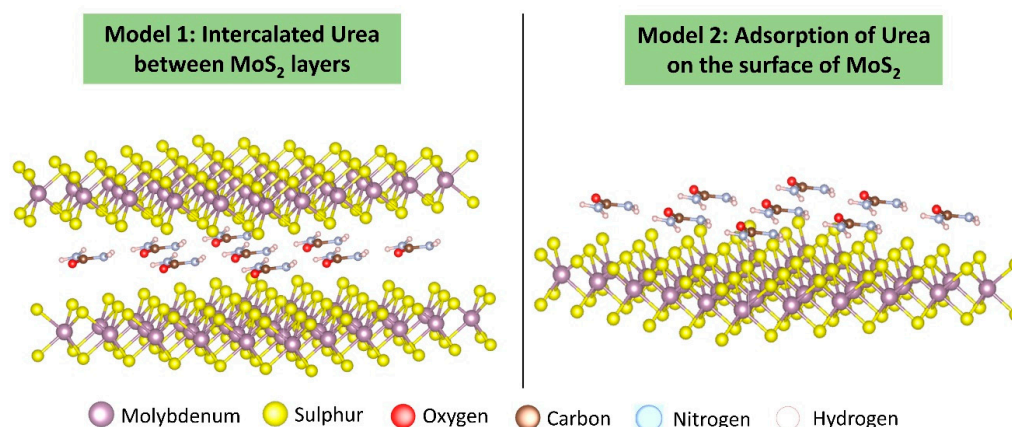


Figure 7. Two different models for the locations of urea molecules within MoS₂ crystals.

Comprehending the crystal structure of U-MoS₂ is essential for elucidating its lubricating mechanism and anticipating its performance attributes. Table 1 presents the results of the geometrical optimization conducted on both MoS₂ and urea-intercalated MoS₂, including the total energy values and their corresponding lattice parameters. The energy subsequent to the intercalation of urea was reduced compared to its pure state, indicating

that the process of urea intercalation exhibits thermodynamic favorability [28,55]. Furthermore, it is worth noting that although there was no alteration in the lattice parameters along the x and y directions after the intercalation of urea into the MoS₂ structure, there was a notable enhancement in the lattice parameter along the Z direction, namely on the (002) plane of the unit cell [56]. This enhancement resulted in an approximate 17 % increase in the volume. The density exhibited a reduction of around 12.5 % as a consequence of the extension of the unit cell. Notably, the enlargement of the unit cell reduces interlayer interactions, facilitating lubrication by promoting smooth sliding between the layers [29,54].

Table 1. Total energies and the geometrical changes in MoS₂ and U-MoS₂.

Compounds	Energy (Ry)	Lattice Parameters		Volume (Å ³)	Density (g/cm ³)
		a(Å)	c(Å)		
MoS ₂	−2890.48	3.183	13.494	118.734	4.477
U-MoS ₂	−2978.23	3.179	15.838	138.954	3.916

The impact of urea's interaction with MoS₂ layers on its molecular structure was examined to understand its implications for the structural stability of urea molecules. According to the data presented in Table 2, the bond lengths and bond angles of urea did not exhibit substantial alterations following its contact with MoS₂ layers. This suggests that the interaction between the urea molecule and MoS₂ layers had no discernible impact on the structural stability of urea [57]. This finding aligns with previous literature reports on the interaction between graphene and urea [32]. In the same manner, the bond length between the elements molybdenum (Mo) and sulfur (S) exhibited a reasonable alteration, decreasing from 2.41 Å to 2.37 Å in response to the intercalation of a urea molecule within the crystal structure of MoS₂. The observed phenomenon can be ascribed to a reduction in interlayer interaction within the MoS₂ crystal structure.

Table 2. The bond lengths and bond angles of the intercalated urea in MoS₂.

	Bond Lengths (Å)				Bond Angles (°)		
	C=O	C-N	N-H	O-C-N	N-C-N	C-N-H	H-N-H
This Study	1.242	1.374	1.007	122.495	113.576	118.642	118.695
Reference [57]	1.221	1.378	1.021	122.64	114.71	119.21	118.61

Furthermore, adsorption energy measures the strength of interaction between a molecule and a surface, indicating how strongly the molecule adheres to the surface and revealing the intermolecular forces at play. Referring to model 2 depicted in Figure 7, the adsorption energy of the urea molecule was calculated using Equation (2), with the results presented in Table 3. Three distinct functionals were employed in DFT calculations to investigate the fluctuations of adsorption energy. In all instances, the energy displayed a negative value and revealed similarity to specific hexagonal layered structures, such as boron nitride (BN), graphene, and oxygen-terminated titanium carbide MXene (O-Ti₃C₂T_x) [31,32,53]. A negative value of adsorption energy signifies a favorable adsorption process, implying that the adsorption of a molecule onto a surface is an energy-releasing, spontaneous event.

Table 3. The calculated adsorption energy of urea on MoS₂ using different functionals.

Compound	MoS ₂ This Study			BN-Nanotube [31]	Graphene [32]	O-Ti ₃ C ₂ T _x [53]
	Functional	GGA-PW91	GGA-PBE	LDA-CA-PZ	GGA-PW91	GGA-PBE
Adsorption Energy (eV)	−0.659	−0.561	−0.681	−0.325	−0.776	−0.530

3.4. Roles of Layered Structure in Tribo-Performance

The MoS₂ layer comprises two planes of sulfur atoms that are covalently connected with a hexagonal plane of molybdenum atoms. The bonding between these layers is assisted by relatively weak van der Waals interactions. The formation of a tribofilm on the steel surface by MoS₂ layers is contingent upon two primary mechanisms: establishing a bond with the steel and facilitating the sliding of MoS₂ layers to disperse onto the substrate [18,27]. In the presence of substantial stress, the sulfur atoms located at the outermost edges of MoS₂ interact with the steel surface, leading to their adhesion onto the surface. The van der Waals connection between the layers is overcome by applied shear stress, which enables the layers to slide away from the bulk and subsequently disperse onto the surface of the steel.

The ability of the layers of MoS₂ to slide depends on applying a specific magnitude of shear force to counteract the van der Waals force. The magnitude of this force is directly influenced by the interlayer distance of the MoS₂ particles [58,59]. The van der Waals interaction between two atoms demonstrates a relationship that is inversely proportional to the sixth power of the distance separating them. [30,60]. Urea molecules intercalate between the layers of MoS₂, expanding the interlayer distance. Based on the results of DFT calculations, the interlayer distance rises from 6.8 Å to 9.45 Å and 7.27 Å at the centered and side positions, respectively, as depicted in Figure 8. The augmentation of the interlayer spacing can effectively reduce the van der Waals forces, hence facilitating the relative movement of the MoS₂ layers. As a result, the development of a tribofilm composed of MoS₂ has a greater chance of being facilitated. Moreover, the presence of nonpolar sulfur atoms within the MoS₂ structure confers hydrophobic characteristics [39–41]. Consequently, it is unable to undergo interactions that would facilitate the formation of bonds with the hydrophilic steel surface spontaneously, resulting in a lack of sustained tribofilm formation. The implantation of urea onto the surface of MoS₂ has the potential to induce a transition from hydrophobic to hydrophilic characteristics. This process facilitates the adhesion of MoS₂ onto the steel surface, resulting in the formation of a resilient tribofilm, as visually portrayed in Figure 8.

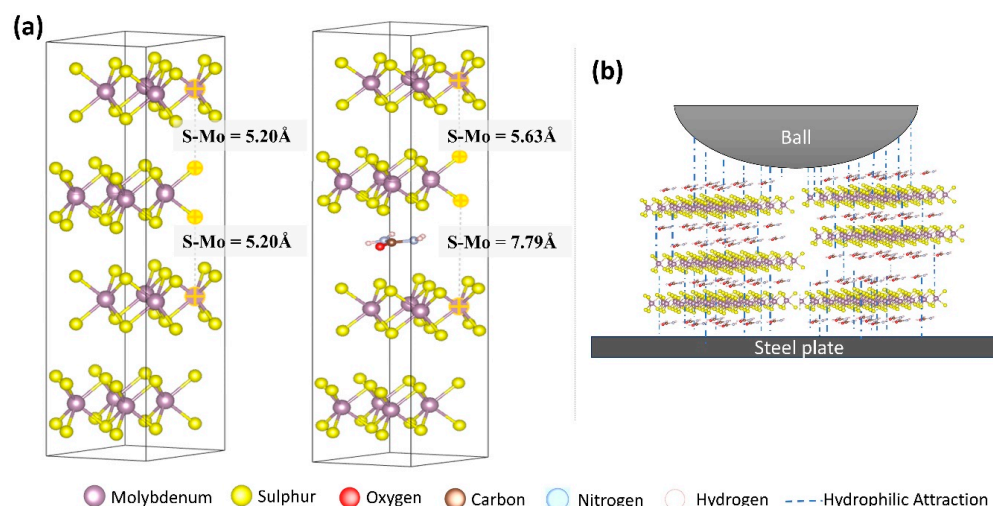


Figure 8. Proposed mechanisms for improving antiwear tribofilm: (a) interlayer distance enhancement; (b) hydrophobic-to-hydrophilic nature conversion.

4. Conclusions

In this study, MoS₂ particles underwent a modification process by interacting with urea molecules to employ an ecologically friendly, low-temperature adsorption reaction. The verification of the existence of urea in MoS₂ was confirmed through thermogravimetric analysis and the X-ray diffraction method. The introduction of urea has the ability to induce a significant transformation in the surface properties of MoS₂, shifting it from a

hydrophobic state to a hydrophilic state, as evidenced by the results of the water dispersibility experiment. The results of tribo-testing demonstrate that the inclusion of 0.25 wt.% U-MoS₂ as an additive in lithium-based grease leads to a substantial reduction in both the friction coefficient and wear rate. The findings from DFT calculations indicate that the thermodynamic stability of MoS₂ is contingent upon the presence of urea molecules, which can be situated both on the surface and between the layers of the particle. The incorporation of urea resulted in an approximate 17 % increase in the volume of MoS₂, while simultaneously causing a drop in density of roughly 12.5 %. Additionally, the interlayer distance saw a modification from approximately 6.8 Å to 9.45 Å and 7.27 Å at the center and side positions, respectively. The surface alteration and interlayer enlargement resulted in the improved performance of the newly functionalized U-MoS₂. In conclusion, the utilization of hydrophilic derivatization and localized interlayer expansion of MoS₂ presents novel avenues for improving the tribological characteristics of two-dimensional materials.

Author Contributions: Conceptualization, M.H.K. and H.L.; Methodology, M.H.K.; Validation, D.D. and K.A.; Formal analysis, M.H.K., D.D., K.A. and R.B.; Investigation, M.H.K., D.D., K.A. and R.B.; Writing—original draft, M.H.K.; Writing—review & editing, M.H.K., D.D., K.A., R.B., H.-J.S. and H.L.; Supervision, H.-J.S. and H.L. All authors have read and agreed to the published version of the manuscript.

Funding: This research received no external funding.

Data Availability Statement: Data is contained within the article.

Conflicts of Interest: The authors declare no conflict of interest.

References

1. Holmberg, K.; Erdemir, A. Influence of Tribology on Global Energy Consumption, Costs and Emissions. *Friction* **2017**, *5*, 263–284. [[CrossRef](#)]
2. Lugt, P.M. Modern Advancements in Lubricating Grease Technology. *Tribol. Int.* **2016**, *97*, 467–477. [[CrossRef](#)]
3. Mu, L.; Shi, Y.; Ji, T.; Chen, L.; Yuan, R.; Wang, H.; Zhu, J. Ionic Grease Lubricants: Protic [Triethanolamine][Oleic Acid] and Aprotic [Choline][Oleic Acid]. *ACS Appl. Mater. Interfaces* **2016**, *8*, 4977–4984. [[CrossRef](#)] [[PubMed](#)]
4. Cai, M.; Liang, Y.; Zhou, F.; Liu, W. Tribological Properties of Novel Imidazolium Ionic Liquids Bearing Benzotriazole Group as the Antiwear/Anticorrosion Additive in Poly(Ethylene Glycol) and Polyurea Grease for Steel/Steel Contacts. *ACS Appl. Mater. Interfaces* **2011**, *3*, 4580–4592. [[CrossRef](#)] [[PubMed](#)]
5. Arole, K.; Tajedini, M.; Sarmah, A.; Athavale, S.; Green, M.J.; Liang, H. Effects of Ti₃C₂T_z MXene Nanoparticle Additive on Fluidic Properties and Tribological Performance. *J. Mol. Liq.* **2023**, *386*, 122435. [[CrossRef](#)]
6. Chen, Y.; Wang, X.; Han, Z.; Sinyukov, A.; Clearfield, A.; Liang, H. Amphiphilic Zirconium Phosphate Nanoparticles as Tribo-Catalytic Additives of Multi-Performance Lubricants. *J. Tribol.* **2022**, *144*, 071901. [[CrossRef](#)]
7. Wang, Y.; Shi, N.; Liu, M.; Han, S.; Yan, J. Enhanced Thermally Conductive Silicone Grease by Modified Boron Nitride. *Lubricants* **2023**, *11*, 198. [[CrossRef](#)]
8. Dong, Y.; Ma, B.; Xiong, C.; Liu, Y.; Zhao, Q. Study on the Lubricating Characteristics of Graphene Lubricants. *Lubricants* **2023**, *11*, 506. [[CrossRef](#)]
9. Lee, J.H.; Cho, D.H.; Park, B.H.; Choi, J.S. Nanotribology of 2D Materials and Their Macroscopic Applications. *J. Phys. D Appl. Phys.* **2020**, *53*, 393001. [[CrossRef](#)]
10. Liu, J.; Qi, Y.; Li, Q.; Duan, T.; Yue, W.; Vadakkepatt, A.; Ye, C.; Dong, Y. Vacancy-Controlled Friction on 2D Materials: Roughness, Flexibility, and Chemical Reaction. *Carbon* **2019**, *142*, 363–372. [[CrossRef](#)]
11. Guo, Y.; Zhou, X.; Lee, K.; Yoon, H.C.; Xu, Q.; Wang, D. Recent Development in Friction of 2D Materials: From Mechanisms to Applications. *Nanotechnology* **2021**, *32*, 312002. [[CrossRef](#)] [[PubMed](#)]
12. Rejhon, M.; Lavini, F.; Khosravi, A.; Shestopalov, M.; Kunc, J.; Tosatti, E.; Riedo, E. Relation between Interfacial Shear and Friction Force in 2D Materials. *Nat. Nanotechnol.* **2022**, *17*, 1280–1287. [[CrossRef](#)] [[PubMed](#)]
13. Bondarev, A.; Ponomarev, I.; Muydinov, R.; Polcar, T. Friend or Foe? Revising the Role of Oxygen in the Tribological Performance of Solid Lubricant MoS₂. *ACS Appl. Mater. Interfaces* **2022**, *14*, 55051–55061. [[CrossRef](#)] [[PubMed](#)]
14. Baş, H.; Özen, O.; Beşirbeyoğlu, M.A. Tribological Properties of MoS₂ and CaF₂ Particles as Grease Additives on the Performance of Block-on-Ring Surface Contact. *Tribol. Int.* **2022**, *168*, 107433. [[CrossRef](#)]
15. Wu, P.R.; Kong, Y.C.; Ma, Z.S.; Ge, T.; Feng, Y.M.; Liu, Z.; Cheng, Z.L. Preparation and Tribological Properties of Novel Zinc Borate/MoS₂ Nanocomposites in Grease. *J. Alloys Compd.* **2018**, *740*, 823–829. [[CrossRef](#)]
16. Hu, E.Z.; Xu, Y.; Hu, K.H.; Hu, X.G. Tribological Properties of 3 Types of MoS₂ Additives in Different Base Greases. *Lubr. Sci.* **2017**, *29*, 541–555. [[CrossRef](#)]

17. Vazirisereshk, M.R.; Martini, A.; Strubbe, D.A.; Baykara, M.Z. Solid Lubrication with MoS₂: A Review. *Lubricants* **2019**, *7*, 57. [[CrossRef](#)]
18. Xu, D.; Wang, C.; Espejo, C.; Wang, J.; Neville, A.; Morina, A. Understanding the Friction Reduction Mechanism Based on Molybdenum Disulfide Tribofilm Formation and Removal. *Langmuir* **2018**, *34*, 13523–13533. [[CrossRef](#)]
19. Bagi, S.D.; Aswath, P.B. Mechanism of Friction and Wear in MoS₂ and ZDDP/F-PTFE Greases under Spectrum Loading Conditions. *Lubricants* **2015**, *3*, 687–711. [[CrossRef](#)]
20. Afanasiev, P.; Lorentz, C. Oxidation of Nanodispersed MoS₂ in Ambient Air: The Products and the Mechanistic Steps. *J. Phys. Chem. C* **2019**, *123*, 7486–7494. [[CrossRef](#)]
21. Spychalski, W.L.; Pisarek, M.; Szoszkiewicz, R. Microscale Insight into Oxidation of Single MoS₂ Crystals in Air. *J. Phys. Chem. C* **2017**, *121*, 26027–26033. [[CrossRef](#)]
22. Kozbial, A.; Gong, X.; Liu, H.; Li, L. Understanding the Intrinsic Water Wettability of Molybdenum Disulfide (MoS₂). *Langmuir* **2015**, *31*, 8429–8435. [[CrossRef](#)] [[PubMed](#)]
23. Stella, M.; Lorenz, C.D.; Clelia Righi, M. Effects of Intercalated Water on the Lubricity of Sliding Layers under Load: A Theoretical Investigation on MoS₂. *2D Mater.* **2021**, *8*, 035052. [[CrossRef](#)]
24. Levita, G.; Righi, M.C. Effects of Water Intercalation and Tribochemistry on MoS₂ Lubricity: An Ab Initio Molecular Dynamics Investigation. *ChemPhysChem* **2017**, *18*, 1475–1480. [[CrossRef](#)]
25. Wang, Y.; Du, Y.; Deng, J.; Wang, Z. Friction Reduction of Water Based Lubricant with Highly Dispersed Functional MoS₂ Nanosheets. *Colloids Surf. A Physicochem. Eng. Asp.* **2019**, *562*, 321–328. [[CrossRef](#)]
26. Chen, Y.; Renner, P.; Liang, H. A Review of Current Understanding in Tribochemical Reactions Involving Lubricant Additives. *Friction* **2023**, *11*, 489–512. [[CrossRef](#)]
27. Yang, Z.; Guo, Z.; Yuan, C. Effects of MoS₂ Microencapsulation on the Tribological Properties of a Composite Material in a Water-Lubricated Condition. *Wear* **2019**, *432–433*, 102919. [[CrossRef](#)]
28. Rasamani, K.D.; Alimohammadi, F.; Sun, Y. Interlayer-Expanded MoS₂. *Mater. Today* **2017**, *20*, 83–91. [[CrossRef](#)]
29. Xiao, H.; Dai, W.; Kan, Y.; Clearfield, A.; Liang, H. Amine-Intercalated α -Zirconium Phosphates as Lubricant Additives. *Appl. Surf. Sci.* **2015**, *329*, 384–389. [[CrossRef](#)]
30. Dappe, Y.J.; Basanta, M.A.; Flores, F.; Ortega, J. Weak Chemical Interaction and van Der Waals Forces between Graphene Layers: A Combined Density Functional and Intermolecular Perturbation Theory Approach. *Phys. Rev. B Condens. Matter Mater. Phys.* **2006**, *74*, 205434. [[CrossRef](#)]
31. Chermahini, A.N.; Teimouri, A.; Farrokhpour, H. Theoretical Studies of Urea Adsorption on Single Wall Boron-Nitride Nanotubes. *Appl. Surf. Sci.* **2014**, *320*, 231–236. [[CrossRef](#)]
32. Singh, R.; Paily, R. Adsorption of Urea over Transition Metal-Doped Graphene: A DFT Study. *J. Electron. Mater.* **2019**, *48*, 6940–6948. [[CrossRef](#)]
33. Min, C.; He, Z.; Liu, D.; Zhang, K.; Dong, C. Urea Modified Fluorinated Carbon Nanotubes: Unique Self-Dispersed Characteristic in Water and High Tribological Performance as Water-Based Lubricant Additives. *New J. Chem.* **2019**, *43*, 14684–14693. [[CrossRef](#)]
34. Giannozzi, P.; Baroni, S.; Bonini, N.; Calandra, M.; Car, R.; Cavazzoni, C.; Ceresoli, D.; Chiarotti, G.L.; Cococcioni, M.; Dabo, I.; et al. QUANTUM ESPRESSO: A Modular and Open-Source Software Project for Quantum Simulations of Materials. *J. Phys. Condens. Matter* **2009**, *21*, 395502. [[CrossRef](#)]
35. Perdew, J.P.; Burke, K.; Ernzerhof, M. Generalized Gradient Approximation Made Simple. *Phys. Rev. Lett.* **1996**, *77*, 3865–3868. [[CrossRef](#)] [[PubMed](#)]
36. Al-Temimy, A.; Anasori, B.; Mazzio, K.A.; Kronast, F.; Seredych, M.; Kurra, N.; Mawass, M.A.; Raoux, S.; Gogotsi, Y.; Petit, T. Enhancement of Ti₃C₂ MXene Pseudocapacitance after Urea Intercalation Studied by Soft X-ray Absorption Spectroscopy. *J. Phys. Chem. C* **2020**, *124*, 5079–5086. [[CrossRef](#)]
37. Baheri, Y.T.; Maleki, M.; Karimian, H.; Javadpoor, J.; Masoudpanah, S.M. Well-Distributed 1T/2H MoS₂ Nanocrystals in the N-Doped Nanoporous Carbon Framework by Direct Pyrolysis. *Sci. Rep.* **2023**, *13*, 7492. [[CrossRef](#)] [[PubMed](#)]
38. Liu, Q.; Li, X.; He, Q.; Khalil, A.; Liu, D.; Xiang, T.; Wu, X.; Song, L. Gram-Scale Aqueous Synthesis of Stable Few-Layered 1T-MoS₂: Applications for Visible-Light-Driven Photocatalytic Hydrogen Evolution. *Small* **2015**, *11*, 5556–5564. [[CrossRef](#)] [[PubMed](#)]
39. Tang, Y.; Zhang, X.; Choi, P.; Xu, Z.; Liu, Q. Contributions of van Der Waals Interactions and Hydrophobic Attraction to Molecular Adhesions on a Hydrophobic MoS₂ Surface in Water. *Langmuir* **2018**, *34*, 14196–14203. [[CrossRef](#)] [[PubMed](#)]
40. Jaiswal, M.K.; Singh, K.A.; Lokhande, G.; Gaharwar, A.K. Superhydrophobic States of 2D Nanomaterials Controlled by Atomic Defects Can Modulate Cell Adhesion. *Chem. Commun.* **2019**, *55*, 8772–8775. [[CrossRef](#)]
41. Koh, E.; Lee, Y.T. Development of Hybrid Hydrophobic Molybdenum Disulfide (MoS₂) Nanoparticles for Super Water Repellent Self-Cleaning. *Prog. Org. Coat.* **2021**, *153*, 106161. [[CrossRef](#)]
42. Ye, X.; Ma, L.; Yang, Z.; Wang, J.; Wang, H.; Yang, S. Covalent Functionalization of Fluorinated Graphene and Subsequent Application as Water-Based Lubricant Additive. *ACS Appl. Mater. Interfaces* **2016**, *8*, 7483–7488. [[CrossRef](#)] [[PubMed](#)]
43. Vaitkunaite, G.; Espejo, C.; Wang, C.; Thiébaud, B.; Charrin, C.; Neville, A.; Morina, A. MoS₂ Tribofilm Distribution from Low Viscosity Lubricants and Its Effect on Friction. *Tribol. Int.* **2020**, *151*, 106531. [[CrossRef](#)]
44. Rai, Y.; Neville, A.; Morina, A. Transient Processes of MoS₂ Tribofilm Formation under Boundary Lubrication. *Lubr. Sci.* **2016**, *28*, 449–471. [[CrossRef](#)]

45. Dai, W.; Kheireddin, B.; Gao, H.; Kan, Y.; Clearfield, A.; Liang, H. Formation of Anti-Wear Tribofilms via α -ZrP Nanoplatelet as Lubricant Additives. *Lubricants* **2016**, *4*, 28. [[CrossRef](#)]
46. Barboza, A.P.M.; Chacham, H.; Oliveira, C.K.; Fernandes, T.F.D.; Ferreira, E.H.M.; Archanjo, B.S.; Batista, R.J.C.; De Oliveira, A.B.; Neves, B.R.A. Dynamic Negative Compressibility of Few-Layer Graphene, h-BN, and MoS₂. *Nano Lett.* **2012**, *12*, 2313–2317. [[CrossRef](#)]
47. Nehme, G.; Mourhatch, R.; Aswath, P.B. Effect of Contact Load and Lubricant Volume on the Properties of Tribofilms Formed under Boundary Lubrication in a Fully Formulated Oil under Extreme Load Conditions. *Wear* **2010**, *268*, 1129–1147. [[CrossRef](#)]
48. Morina, A.; Neville, A. Tribofilms: Aspects of Formation, Stability and Removal. *J. Phys. D Appl. Phys.* **2007**, *40*, 5476–5487. [[CrossRef](#)]
49. Wang, Q.H.; Kalantar-Zadeh, K.; Kis, A.; Coleman, J.N.; Strano, M.S. Electronics and Optoelectronics of Two-Dimensional Transition Metal Dichalcogenides. *Nat. Nanotechnol.* **2012**, *7*, 699–712. [[CrossRef](#)] [[PubMed](#)]
50. Zhao, W.; Pan, J.; Fang, Y.; Che, X.; Wang, D.; Bu, K.; Huang, F. Metastable MoS₂: Crystal Structure, Electronic Band Structure, Synthetic Approach and Intriguing Physical Properties. *Chem. A Eur. J.* **2018**, *24*, 15942–15954. [[CrossRef](#)]
51. Zhao, Z.Y.; Liu, Q.L. Study of the Layer-Dependent Properties of MoS₂ Nanosheets with Different Crystal Structures by DFT Calculations. *Catal. Sci. Technol.* **2018**, *8*, 1867–1879. [[CrossRef](#)]
52. Krishnan, U.; Kaur, M.; Singh, K.; Kumar, M.; Kumar, A. A Synoptic Review of MoS₂: Synthesis to Applications. *Superlattices Microstruct.* **2019**, *128*, 274–297. [[CrossRef](#)]
53. Meng, F.; Seredych, M.; Chen, C.; Gura, V.; Mikhalovsky, S.; Sandeman, S.; Ingavle, G.; Ozulumba, T.; Miao, L.; Anasori, B.; et al. MXene Sorbents for Removal of Urea from Dialysate: A Step toward the Wearable Artificial Kidney. *ACS Nano* **2018**, *12*, 10518–10528. [[CrossRef](#)]
54. Mashtalir, O.; Naguib, M.; Mochalin, V.N.; Dall’Agnese, Y.; Heon, M.; Barsoum, M.W.; Gogotsi, Y. Intercalation and Delamination of Layered Carbides and Carbonitrides. *Nat. Commun.* **2013**, *4*, 1716. [[CrossRef](#)] [[PubMed](#)]
55. Tang, Y.J.; Wang, Y.; Wang, X.L.; Li, S.L.; Huang, W.; Dong, L.Z.; Liu, C.H.; Li, Y.F.; Lan, Y.Q. Molybdenum Disulfide/Nitrogen-Doped Reduced Graphene Oxide Nanocomposite with Enlarged Interlayer Spacing for Electrocatalytic Hydrogen Evolution. *Adv. Energy Mater.* **2016**, *6*, 1600116. [[CrossRef](#)]
56. Zhang, S.; Yu, X.; Yu, H.; Chen, Y.; Gao, P.; Li, C.; Zhu, C. Growth of Ultrathin MoS₂ Nanosheets with Expanded Spacing of (002) Plane on Carbon Nanotubes for High-Performance Sodium-Ion Battery Anodes. *ACS Appl. Mater. Interfaces* **2014**, *6*, 21880–21885. [[CrossRef](#)]
57. Godfrey, P.D.; Brown, R.D.; Hunter, A.N. The Shape of Urea. *J. Mol. Struct.* **1997**, *413–414*, 405–414. [[CrossRef](#)]
58. Lu, N.; Guo, H.; Zhuo, Z.; Wang, L.; Wu, X.; Zeng, X.C. Twisted MX₂/MoS₂ Heterobilayers: Effect of van Der Waals Interaction on the Electronic Structure. *Nanoscale* **2017**, *9*, 19131–19138. [[CrossRef](#)] [[PubMed](#)]
59. Li, B.; Yin, J.; Liu, X.; Wu, H.; Li, J.; Li, X.; Guo, W. Probing van Der Waals Interactions at Two-Dimensional Heterointerfaces. *Nat. Nanotechnol.* **2019**, *14*, 567–572. [[CrossRef](#)]
60. Gómez-Santos, G. Thermal van Der Waals Interaction between Graphene Layers. *Phys. Rev. B Condens. Matter Mater. Phys.* **2009**, *80*, 245424. [[CrossRef](#)]

Disclaimer/Publisher’s Note: The statements, opinions and data contained in all publications are solely those of the individual author(s) and contributor(s) and not of MDPI and/or the editor(s). MDPI and/or the editor(s) disclaim responsibility for any injury to people or property resulting from any ideas, methods, instructions or products referred to in the content.